

Magnetoelectric coupling in sol-gel synthesized dilute magnetostrictive-piezoelectric composite thin films

Subhasis Roy, Ratnamala Chatterjee, and S. B. Majumder

Citation: *Journal of Applied Physics* **110**, 036101 (2011); doi: 10.1063/1.3610795

View online: <http://dx.doi.org/10.1063/1.3610795>

View Table of Contents: <http://scitation.aip.org/content/aip/journal/jap/110/3?ver=pdfcov>

Published by the [AIP Publishing](#)

Articles you may be interested in

[Converse magnetoelectric coupling in NiFe/Pb\(Mg_{1/3}Nb_{2/3}\)O₃-PbTiO₃ nanocomposite thin films grown on Si substrates](#)

Appl. Phys. Lett. **103**, 192903 (2013); 10.1063/1.4828878

[Optical characteristic of sol-gel synthesized lead lanthanum titanate-cobalt iron oxide multiferroic composite thin film](#)

J. Appl. Phys. **112**, 043520 (2012); 10.1063/1.4747918

[Theoretical model for geometry-dependent magnetoelectric effect in magnetostrictive/piezoelectric composites](#)

J. Appl. Phys. **111**, 124513 (2012); 10.1063/1.4729832

[Magnetoelectric nano- Fe₃O₄/Co Fe₂O₄ Pb Zr_{0.53} Ti_{0.47} O₃ composite](#)

Appl. Phys. Lett. **92**, 083502 (2008); 10.1063/1.2841064

[Orientation-dependent multiferroic properties in Pb \(Zr_{0.52} Ti_{0.48} \) O₃ - Co Fe₂ O₄ nanocomposite thin films derived by a sol-gel processing](#)

J. Appl. Phys. **103**, 034103 (2008); 10.1063/1.2838482



Magnetolectric coupling in sol-gel synthesized dilute magnetostrictive-piezoelectric composite thin films

Subhasis Roy,¹ Ratnamala Chatterjee,² and S. B. Majumder^{1,a)}

¹Materials Science Centre, IIT Kharagpur 721302, India

²Advanced Ceramic Laboratory, Department of Physics, IIT Delhi 110016, India

(Received 18 May 2011; accepted 18 June 2011; published online 3 August 2011)

Multiferroic lead lanthanum titanate–cobalt iron oxide nano-composite thin films are synthesized by sol-gel route. A percolative distribution of cobalt iron oxide phase, with percolation threshold ~ 8 vol%, is identified in these films. Large magnetolectric coupling coefficient (~ 250 mV/cm.Oe) is found in the composite films with cobalt iron oxide volume contents in the vicinity of its percolation threshold. The composite films with dilute magnetostrictive volume contents yield superior multiferroic properties to its counterparts with relatively higher magnetostrictive volume contents. © 2011 American Institute of Physics. [doi:10.1063/1.3610795]

Product property based magnetostrictive: piezoelectric composite thin films with large magnetolectric coupling coefficient are attractive for many practical applications.¹ Using various theoretical formalisms it is predicted that 1-3 type vertical heterostructure with low leakage current would yield large magnetolectric coupling coefficient²⁻⁴ whereas 2-2 type laminated composites would yield poor coupling coefficient due to substrate constraint effect.⁵

0-3 type composite thin films are synthesized by physical vapor deposition and chemical solution deposition techniques.⁶⁻¹¹ A number of unanswered questions have emerged through these literature reports that can be grouped as follows: (1) how to synthesize such 0-3 type nano-composite thin films? Is it ideal to disperse the crystalline magnetostrictive phase content in piezoelectric precursor and deposit these films by spin coating, or to mix the precursor solutions of magnetostrictive and piezoelectric components at molecular level and spin coat the mixed solution? (2) It is interesting to investigate whether the magnitude of the magnetolectric coupling coefficient of the composite thin film is dependent on the volume ratio of magnetostrictive and piezoelectric phase contents and if yes then what would be the optimized ratio that yield maximum magnetolectric coupling coefficient? Finally, (3) it is worth investigating how (a) the dc conductivity, (b) electric polarization, (c) magnetization, (d) frequency dispersion of dielectric constant and loss tangent varies with the volume ratio of magnetostrictive and piezoelectric phase contents?

In this work we demonstrate that homogeneous distribution of magnetostrictive phase in piezoelectric matrix (0-3 type) could be a better alternative than the 1-3 or 2-2 thin film configuration to circumvent the problem of leakage and substrate constrain, respectively.

The details of the synthesis of $(1-x)\text{Pb}_{0.85}\text{La}_{0.15}\text{TiO}_3$ (PLT15)- $x\text{CoFe}_2\text{O}_4$ (CFO) [x , volume fraction of CFO $\sim 0.0, 0.012, 0.036, 0.059, 0.083, \text{ and } 0.117$] composite thin films are described elsewhere.¹¹ The annealed films were characterized in terms of their phase formation behavior and microstructure evolution using an X-ray diffractometer (XRD)

and field emission scanning electron microscope (FESEM) equipped with energy dispersive spectrometer (EDS) respectively. The dielectric properties of these films are characterized using a LCR meter. The ferroelectric and magnetic characteristics of these films are characterized using a ferroelectric tester and vibrating sample magnetometer respectively. To measure ME coefficient (dE/dH), the composite films were put in a dc magnetic field that was varied up to 3 kOe. The measurements were done with superimposed small amplitude of ac magnetic fields generated by Helmholtz coils. Both ac and dc magnetic fields were kept parallel to the direction of polarization (longitudinal mode). The output voltage generated by the composite film was measured using SR-830 lock in amplifier.

PLT15 film was crystallized into desired perovskite structure. The details of the phase formation behavior is already published in one of our recent publications.¹¹ Figure 1 shows surface and cross sectional morphology of PLT15 [Figs. 1(a) and 1(b)], PLT15-CFO (~ 6.0 vol%) [Figs. 1(c) and 1(d)], and PLT15-CFO (~ 12.0 vol%) [Figs. 1(e) and 1(f)] composite thin films. PLT15 thin film exhibit dense and homogeneous microstructure and rosette-type grain morphology common to sol-gel derived perovskite films.¹² In the PLT15-CFO composite films, CFO grains (black regions, confirmed by EDS) are found to be uniformly dispersed in PLT15 matrix. The cross sectional surface morphologies of both PLT15 and PLT15-CFO (~ 6.0 vol%) composite films are equiaxed [see Figs. 1(b) and 1(d)], however, it changes to columnar type in PLT15-CFO (12.0 vol%) composite film [Fig. 1(f)].

The composite films exhibit both polarization and magnetic hysteresis loops at room temperature.

For these films, the measured dielectric constant and loss tangent maximize at certain specific CFO volume contents and then decreased steadily. This is in contrary to many literatures reports where a monotonic decrease of the dielectric constant of such composite film or bulk composite is reported with the increase in CFO volume contents.^{13,14} The dc conductivity of the composite films is found to increase monotonically with the increase in CFO volume contents. According to a general percolation theory developed for ceramic-metal composite,¹⁵ the dielectric constant of a composite is strongly dependent on the conductivity ratio of the matrix and dispersed phase. For

^{a)}Author to whom correspondence should be addressed: Electronic mail: subhasish@matsc.iitkgp.ernet.in.

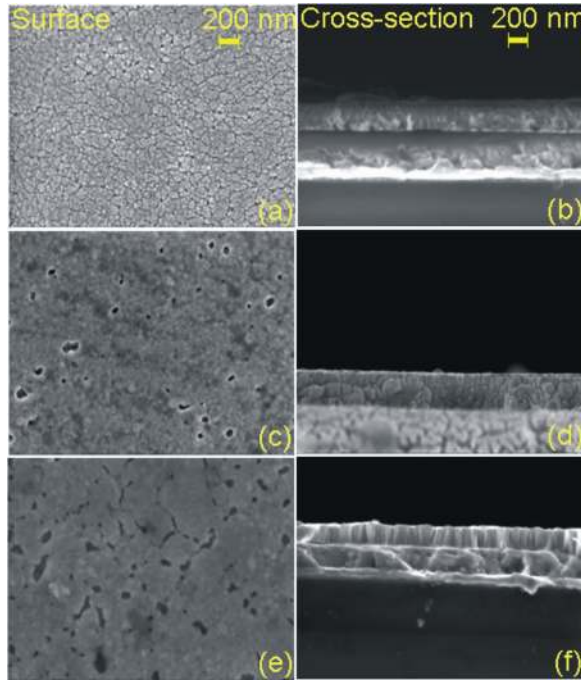


FIG. 1. (Color online) (a) Surface and (b) cross sectional morphology of $\text{Pb}_{0.85}\text{La}_{0.15}\text{TiO}_3$, (c) surface and (d) cross sectional surface morphology of $0.92 \text{Pb}_{0.85}\text{La}_{0.15}\text{TiO}_3-0.08 \text{CoFe}_2\text{O}_4$ and (e) surface and (f) cross sectional surface morphology of $0.88 \text{Pb}_{0.85}\text{La}_{0.15}\text{TiO}_3-0.12 \text{CoFe}_2\text{O}_4$ thin films.

such percolative composites the following relations are valid for $V_{\text{CFO}} < V_{\text{CFO}}^c$:¹⁶

$$\varepsilon_{\text{comp}} = \varepsilon_{\text{PLT15}} \left[\frac{(V_{\text{CFO}}^c - V_{\text{CFO}})}{V_{\text{CFO}}^c} \right]^{-q} \quad (1)$$

$$\tan \delta_{\text{comp}} = \tan \delta_{\text{PLT15}} \left[\frac{(V_{\text{CFO}}^c - V_{\text{CFO}})}{V_{\text{CFO}}^c} \right]^{-n'}. \quad (2)$$

$$\sigma_{\text{comp}} = \sigma_{\text{PLT15}} \left[\frac{(V_{\text{CFO}}^c - V_{\text{CFO}})}{V_{\text{CFO}}^c} \right]^{-q'} \quad (3)$$

where $\varepsilon_{\text{comp}}$, $\tan \delta_{\text{comp}}$, σ_{comp} and $\varepsilon_{\text{PLT15}}$, $\tan \delta_{\text{PLT15}}$, σ_{PLT15} are the relative dielectric constant, loss tangent, and conductivity of the composite and PLT15 thin films respectively. V_{CFO} , V_{CFO}^c are the volume content of CFO and its percolation threshold respectively and q , n' , and q' are the critical exponent for dielectric constant, loss tangent and conductivity. As shown in Fig. 2 for $V_{\text{CFO}} < V_{\text{CFO}}^c$, the variation of the dielectric constant, loss tangent and dc conductivity fits well to Eqs. (1)–(3) and there is a good agreement between V_{CFO}^c derived from dielectric and conductivity data.

The percolative dielectric properties in ceramic: metal composite has been proposed to be due to the formation of random micro-capacitor and/or Maxwell-Wagner polarization.¹⁷ Due to the remarkable difference in the dielectric permittivity and conductivity between PLT15 and CFO phases together with their nano-scale mixing could lead to Maxwell-Wagner polarization.¹² The frequency dispersion of real ($\varepsilon'_{\text{comp}}$) and imaginary part ($\varepsilon''_{\text{comp}}$) of the dielectric constant can be represented by the following equations.¹⁶

$$\begin{aligned} \varepsilon'_{\text{comp}}(\omega) = & [K_{\sigma} [\sigma_{\text{PLT15}} \{ (1 - V_{\text{CFO}}) / V_{\text{CFO}}^c \}^{-q'}] / \varepsilon_0 \omega^{1-n}] \\ & + \{ (1 - V_{\text{CFO}}) / V_{\text{CFO}}^c \}^{-u} [(\varepsilon_{\alpha\text{PLT15}} \\ & + [\varepsilon_{\text{sPLT15}} - \varepsilon_{\alpha\text{PLT15}}] / [1 + \omega^2 \tau^2]), \end{aligned} \quad (4)$$

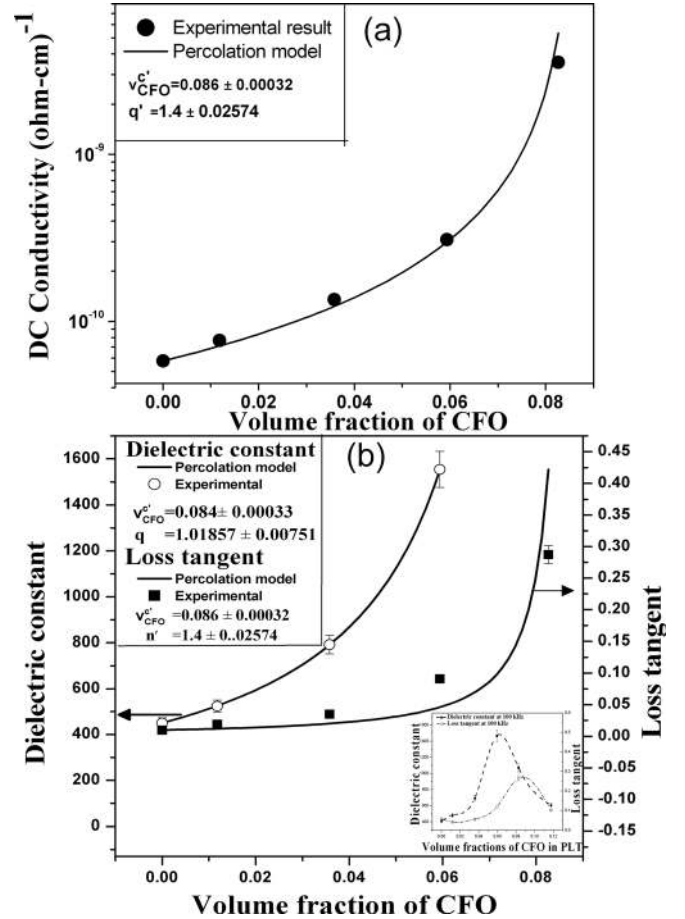


FIG. 2. Variation of (a) the dc conductivity and (b) the dielectric constant/loss tangent of PLT15-CFO composite thin films with CFO volume contents. The symbols represent the experimental data and the solid lines are the non-linear best fit based on Eq. (1) (for dielectric constant), Eq. (2) (for loss tangent) and Eq. (3) (for dc conductivity), respectively. The best fitted parameters are indicated in the inset of the respective figures. The inset shows the variation of the dielectric constant and loss tangent with CFO volume contents ranging from 0.0 to 12.0 vol% in PLT-15-CFO composite films.

$$\begin{aligned} \varepsilon''_{\text{comp}}(\omega) = & [(\sigma_{\text{PLT15}} \{ (1 - V_{\text{CFO}}) / V_{\text{CFO}}^c \}^{-q'}) / \varepsilon_0 \omega^{1-n}] \\ & + \{ (1 - V_{\text{CFO}}) / V_{\text{CFO}}^c \}^{-u} [(\varepsilon_{\text{sPLT15}} \\ & - \varepsilon_{\alpha\text{PLT15}}) \omega \tau] / [1 + \omega^2 \tau^2]. \end{aligned} \quad (5)$$

Where $\varepsilon'_{\text{comp}}(\omega)$ and $\varepsilon''_{\text{comp}}(\omega)$ real and imaginary part of dielectric constant, ω -measurement frequency, $K_{\sigma} = \tan(n\pi/2)$, σ_{PLT15} -conductivity of pure PLT15, V_{CFO} -volume fraction of CFO, V_{CFO}^c percolation threshold, ε_0 -dielectric permittivity of free space, n -frequency exponent ($0 < n < 1$), q' and u are critical exponent to conductivity and dielectric constant, ω is the angular frequency, τ is the relaxation time, and $\varepsilon_{\text{sPLT}}$ and $\varepsilon_{\alpha\text{PLT}}$ are the dielectric constant of PLT15 at ultra low and ultrahigh frequency respectively. For 0.92 PLT15-0.08CFO composite thin film, Fig. 3 shows [Fig. 3(a)] the real and [Fig. 3(b)] imaginary part of the dielectric constant (symbol) and the best fitted curve (solid line) based on Eqs. (4) and (5), respectively. Note that in these fitting we have kept only 5 parameters (namely V_{CFO}^c , n ($0 < n < 1$), q' , u , and τ) free. Similar to the results presented in Fig. 3, excellent fit is also obtained for other composite film at $V_{\text{CFO}} < V_{\text{CFO}}^c$. These results support the percolative model of the magnetostrictive

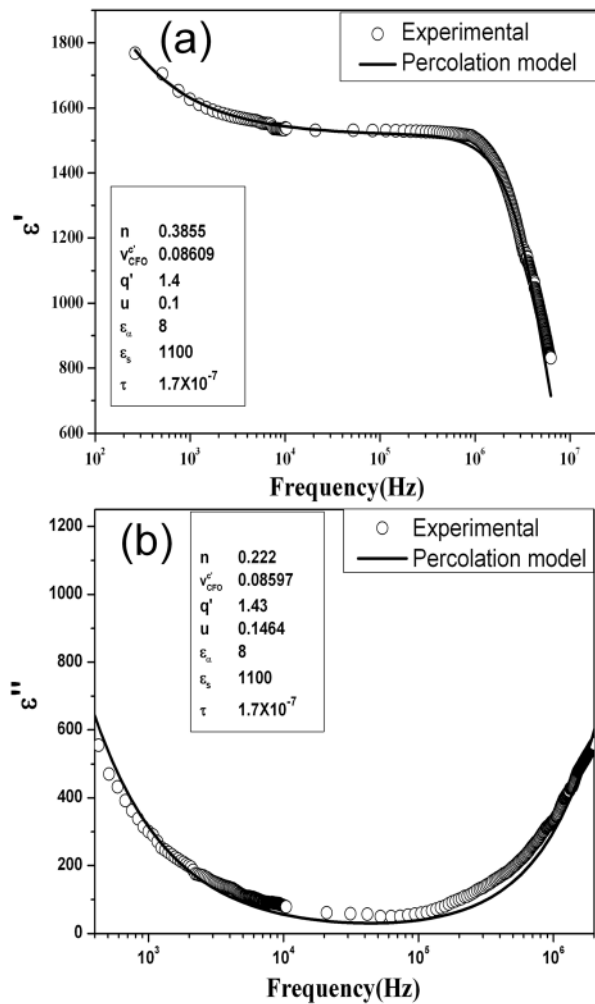


FIG. 3. Frequency dispersion of (a) the real and (b) imaginary part of dielectric constant of 0.92 $\text{Pb}_{0.85}\text{La}_{0.15}\text{TiO}_3$ -0.08 CoFe_2O_4 composite thin film. The symbols represent the experimental data and the solid lines are the non-linear best fit based on Eq. (4) for real, and Eq. (5) for imaginary part of the dielectric constant. The relevant best fitted parameters are indicated in the inset of the respective figures.

phase and a space-charge as well as dipolar polarization base hybrid dielectric response in these composite films.

Maximum magnetoelectric coupling coefficient (α_{\max}) is obtained at optimized dc magnetic field. Figure 4 shows the variation of estimated α_{\max} with CFO volume contents at three different ac frequencies. It is interesting to note that α_{\max} is significantly increased in composite film with CFO volume content in the vicinity (within 2.0 vol% of CFO contents) of the percolation threshold. With further increase in CFO volume contents α_{\max} drops and probably levels off. Thus for $x \sim 0.06$, α_{\max} is measured to be ~ 250 mV/cm.Oe (at 20 kHz). As compared to the magnetoelectric coupling coefficients reported for other 0-3 type composite films ($\alpha = 34.5$ mV/cm.Oe for $0.5\text{Bi}_{3.15}\text{Nd}_{0.85}\text{Ti}_3\text{O}_{12}$ - $0.5\text{CoFe}_2\text{O}_4$; $\alpha = 30$ mV/cm.Oe for PZT: CoFe_2O_4 ; and $\alpha = 16$ mV/cm.Oe for PZT: NiFe_2O_4)^{8,18,19} as well as ferroelectric (PZT)-ferrite (CoFe_2O_4) multilayered films ($\alpha = 15$ mV/cm.Oe),¹⁰ our films yield significantly large magnetoelectric coupling coefficients.

In the present work, using a mixed precursor sol, we have synthesized $(1-x)\text{Pb}_{0.85}\text{La}_{0.15}\text{TiO}_3 - x\text{CoFe}_2\text{O}_4$ ($x, \sim 0.0$ to

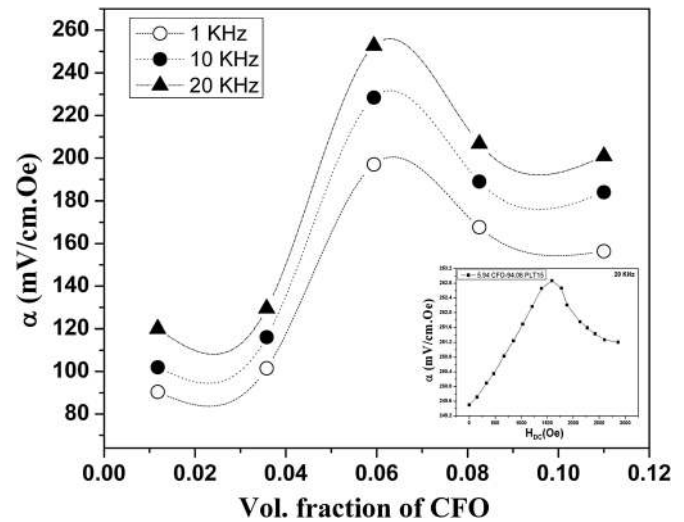


FIG. 4. Variation of the estimated α_{\max} with CFO volume contents at various frequencies of the applied ac magnetic field. The inset shows the variation of the magnetoelectric coupling coefficient of 94.06 PLT15-5.94 CFO composite film with the dc bias magnetic field (measured at 20 kHz).

12%) composite thin films by sol-gel route. Through the analyses of dc conductivity, frequency dispersion of dielectric constant and loss tangent percolative nature of cobalt iron oxide in lead lanthanum titanate matrix has clearly been demonstrated. In the vicinity of the percolation threshold magnetoelectric coupling coefficient maximum is reported to be ~ 250 mV/cm. Oe. These composite films with dilute magnetostrictive volume contents are argued to be superior to similar films with relatively higher magnetostrictive volume contents.

- ¹J. Ma, J. Hu, Z. Li, and C-W Nan, *Adv. Mater* **23**, 1062 (2011).
- ²C. W. Nan, G. Liu, Y. H. Liu, and H. D. Chen, *Phys. Rev. Lett.* **94**, 197203 (2005).
- ³V. M. Petrov, M. I. Bichurin, and G. Srinivasan, *J. Appl. Phys.* **107**, 073908 (2010).
- ⁴P. P. Wu, X. Q. Ma, J. X. Zhang, and L. Q. Chen, *Philos. Mag.* **90**, 125 (2010).
- ⁵H. Zheng, J. Wang, S. E. Lofland, Z. Ma, L. M. Ardabili, T. Zhao, L. S. Riba, S. R. Shinde, S. B. Ogale, F. Bai, D. Viehland, Y. Jia, D. G. Schlom, M. Wuttig, A. Roytburd, and R. Ramesh, *Science* **303**, 661 (2004).
- ⁶Y. Wang, J. Hu, Y. Lin, and C-W Nan, *NPG Asia Mater.* **2**, 61 (2010).
- ⁷M. Murakami, K.-S. Chang, M. A. Aronova, C.-L. Lin, M. H. Yu, H. Simpers, M. Wuttig, I. Takeuchi, C. Gao, B. Hu, S. E. Lofland, L. A. Knauss, and L. A. Bendersky, *Appl. Phys. Lett.* **87**, 112901 (2005).
- ⁸X. L. Zhong, J. B. Wang, M. Liao, G. J. Huang, S. H. Xie, Y. C. Zhou, Y. Qiao, and J. P. He, *Appl. Phys. Lett.* **90**, 152903 (2007).
- ⁹M. Liu, X. Li, J. Lou, S. Zheng, K. Du, and N. X. Sun, *J. Appl. Phys.* **102**, 083911 (2007).
- ¹⁰H.-C. He, J. Ma, J. Wang, and C.-W. Nan, *J. Appl. Phys.* **103**, 034103 (2008).
- ¹¹S. Roy and S. B. Majumder, *Phys. Lett. A* **375**, 1538 (2011).
- ¹²S. Bhaskar, S. B. Majumder, M. Jain, P. S. Dopal, and R. S. Katiyar, *Mater. Sci. Eng. B* **87**, 178 (2001).
- ¹³H.-C. He, J. Ma, Z. Li, and C-W Nan, *J. Appl. Phys.* **104**, 114114 (2008).
- ¹⁴Y. Zhou, J. Zhang, L. Li, Y. Su, J. Cheng, and S. Cao, *J. Alloys Compd.* **484**, 535 (2009).
- ¹⁵S. Kirkpatrick, *Rev. Mod. Phys.* **45**, 574 (1973).
- ¹⁶Z. Chen, J. Huang, Q. Chen, C. Song, G. Han, W. Weng, and P. Du, *Scr. Mater.* **57**, 921 (2007).
- ¹⁷J. Huang, Y. Cao, M. Hong, and P. Du, *Appl. Phys. Lett.* **92**, 022911 (2008).
- ¹⁸J.-G. Wan, H. Zhang, X. Wang, D. Pan, J.-M. Liu, and G. Wang, *Appl. Phys. Lett.* **89**, 122914 (2006).
- ¹⁹S. Ryu, P. Murugavel, J. H. Lee, S. C. Chae, T. W. Noh, Y. S. Oh, H. J. Kim, K. H. Kim, J. H. Jang, M. Kim, C. Bae, and J.-G. Park, *Appl. Phys. Lett.* **89**, 102907 (2006).